PROCEEDINGS, 48th Workshop on Geothermal Reservoir Engineering
Stanford University, Stanford, California, February 6-8, 2023
SGP-TR-224

Experimental and Numerical Study of Hydraulic Fracturing in Enhanced Geothermal Systems (EGS)

Fan Fei[a], Yunxing Lu[b], Andrew P. Bunger[b,c] and Matteo Cusini[a]

[a]Atmospheric, Earth, and Energy Division, Lawrence Livermore National Laboratory, USA

[b]Department of Civil and Environmental Engineering, University of Pittsburgh, USA

[c]Department of Chemical and Petroleum Engineering, University of Pittsburgh, USA

E-mail address: fei2@llnl.gov

Keywords: Near-wellbore hydraulic fracturing, hydraulic fracturing experiment, true triaxial stress, phase-field simulation

ABSTRACT

Enhanced Geothermal Systems (EGS) rely on hydraulic fracturing to enhance the hydraulic conductivity of nearly impermeable subsurface formations. The propagation patterns of hydraulic fractures and their reactivation are dictated by several factors, such as rock heterogeneities, temperature variations, and in-situ stress magnitude and orientations. Thus, to perform effective stimulation and ensure long term performance of EGS, it is crucial to understand the influence of these factors on the hydraulic fracturing process. In this work, we present initial results from a combined experimental and numerical study of near-wellbore hydraulic fracture propagation. The laboratory investigation entails a series of hydraulic fracturing experiments on cold spring granite samples under a true triaxial stress condition, in which we can obtain the breakdown pressure, fracture geometry, and re-opening pressure. These experimental results are used to calibrate a phase-field numerical model for hydraulic fracture initiation and propagation. The calibrated model is then employed to explore the effect of the in-situ stress on the hydraulic fracturing process. The outcome of this combined study is believed to advance our understanding of the reservoir-scale hydraulic fracturing process in EGS.

1. INTRODUCTION

Hydraulic fracturing is a well stimulation technique commonly applied in Enhanced Geothermal Systems (EGS) to enhance the permeability of the target formations that are otherwise too impermeable to allow for sufficient fluid circulation. The effectiveness of the hydraulic fracturing treatment strongly depends on the behavior of fractures generated in the near-wellbore region. Therefore, understanding the mechanism behind nucleation and propagation of near-wellbore hydraulic fractures is essential for the design of a successful hydraulic fracturing scheme.

Prior studies have evidenced that nucleation and propagation of hydraulic fractures in the near-wellbore region are influenced by a number of factors. One notable example is the in-situ stress condition. In fact, a non-preferred in-situ stress regime may give rise to the reorientation of hydraulic fractures nucleated from the wellbore, and further lead to near-wellbore fracture tortuosity (Hossain et al., 2000; Zhang et al., 2011). This fracture tortuosity has been recognized as the cause of many critical issues observed in the hydraulic fracturing practice, such as premature screen-outs and low proppant concentration (Cleary et al., 1993). Also, analytical studies (Haimson and Fairhurst, 1967; Hossain et al., 2000) have shown that the in-situ stress condition determines the stress distribution around the wellbore, which influences the fracture initiation pressure. These observations have motivated us to carry out a fundamental analysis of the near-wellbore hydraulic fracturing process under various in-situ stresses.

For this purpose, we conduct a combined experimental and numerical study to investigate the near-wellbore nucleation and propagation of hydraulic fractures. Here, we present both our experimental and our modeling capabilities and our initial results. We conduct a laboratory-scale hydraulic fracturing experiment which consists in injecting a fluid through a cylindrical borehole into a cubic sample of granite subject to true triaxial loading stress conditions. Based on the experimental observation, we subsequently perform a numerical investigation to explore how the fracture geometry and fracture initiation pressure is affected by the in-situ stress.

The numerical method employed in this work is a phase-field model, specifically developed by some of the authors of this work for hydraulic fracture nucleation and propagation in rocks. In general, phase-field is an appealing approach to modeling fracture propagation as it does not require to explicitly track the evolution of the fractures geometry (Miehe et al., 2010; Borden et al., 2012; Fei and Choo, 2020; Fei and Choo, 2021). Thus, over the past decade, phase-field approaches have become more popular among the computational geoscience community to model hydraulic fracturing processes (Wheeler et al., 2014; Mikelic et al., 2015; Santillan et al., 2018; Chukwudozie et al., 2019). Remarkably, the particular phase-field formulation adopted in this paper has the unique advantage of incorporating rock strengths. As a consequence, it can correctly predict the fracture initiation pressure due to fracture nucleation in the bulk. Thus, we believe this phase-field formulation provides a reliable numerical investigation tool.

The paper is organized as follows. Section 2 provides the specific design and results of the hydraulic fracturing experiment conducted so far. Section 3 introduces the phase-field method and calibrates the modeling parameters according to the experimental data. Using the

calibrated model, we further perform a series of numerical tests with different in-situ stress conditions. The fracture initiation pressure and crack propagation patterns obtained through the numerical investigation are presented and discussed. Section 4 concludes this work.

2. EXPERIMENTAL INVESTIGATION

This section introduces the samples, apparatus, and procedures for the hydraulic fracturing experiment. Experimental results are subsequently presented in terms of the wellbore pressure evolution and fracture pattern.

2.1 Experimental Design and Samples

In this experimental study, we aim to generate hydraulic fractures by injecting fluids into a Cold Spring Charcoal Granite sample that is under a true triaxial compression state. The sample is sourced from the quarry after which it is fabricated into 8-inch cubic blocks with flat, square, and parallel faces. A vertical cylindrical wellbore is drilled through the sample from one face center to the opposite one. Here, we consider two cases with different wellbore orientations relative to the wave speed anisotropy of the sample, which is obtained from the acoustic velocity measurements. Specifically, Test 1 has the wellbore orientation aligned with the direction of the minimum wave speed, while Test 2 has the wellbore orientation aligned with the direction of the maximum wave speed.

The sample is then loaded in a true triaxial stress condition, in which all stress components are different.

(a)

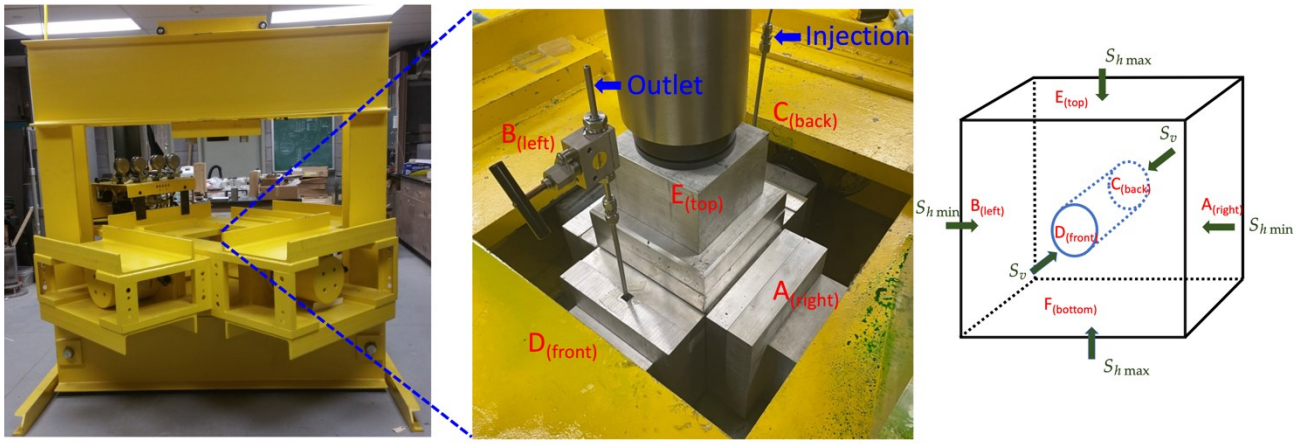

(b)

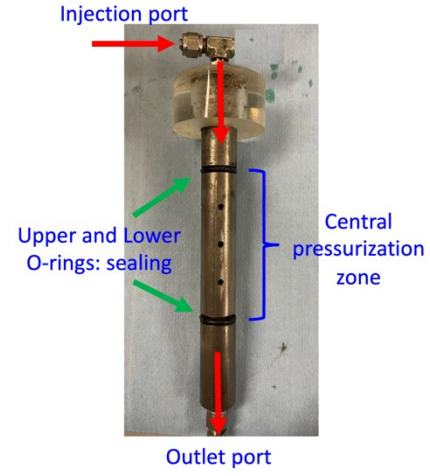

Figure 1(a) presents the triaxial loading frame that utilizes a hydraulic piston-actuated loading cell to independently control the stresses in all three axes. The orientation of each in-situ stress component relative to the wellbore is shown in the right of Figure 1(a). Here, we consider that the in-situ stress condition lies in a normal stress regime, in which the vertical stress S_v along the wellbore direction (C-D orientation) has the largest magnitude, which is 17.5 MPa. The maximum horizontal stress $S_{h\,max}$ (E-F orientation) and minimum horizontal stress $S_{h\,min}$ (A-B orientation) are both perpendicular to the wellbore direction and have magnitudes of 15 MPa and 10 MPa, respectively. To ensure an even stress distribution on the sample, we insert aluminum loading plates with thickness of at least 3 inch between each surface of the sample and the tilt saddle on the actuator, as illustrated in the middle of Figure 1(a).

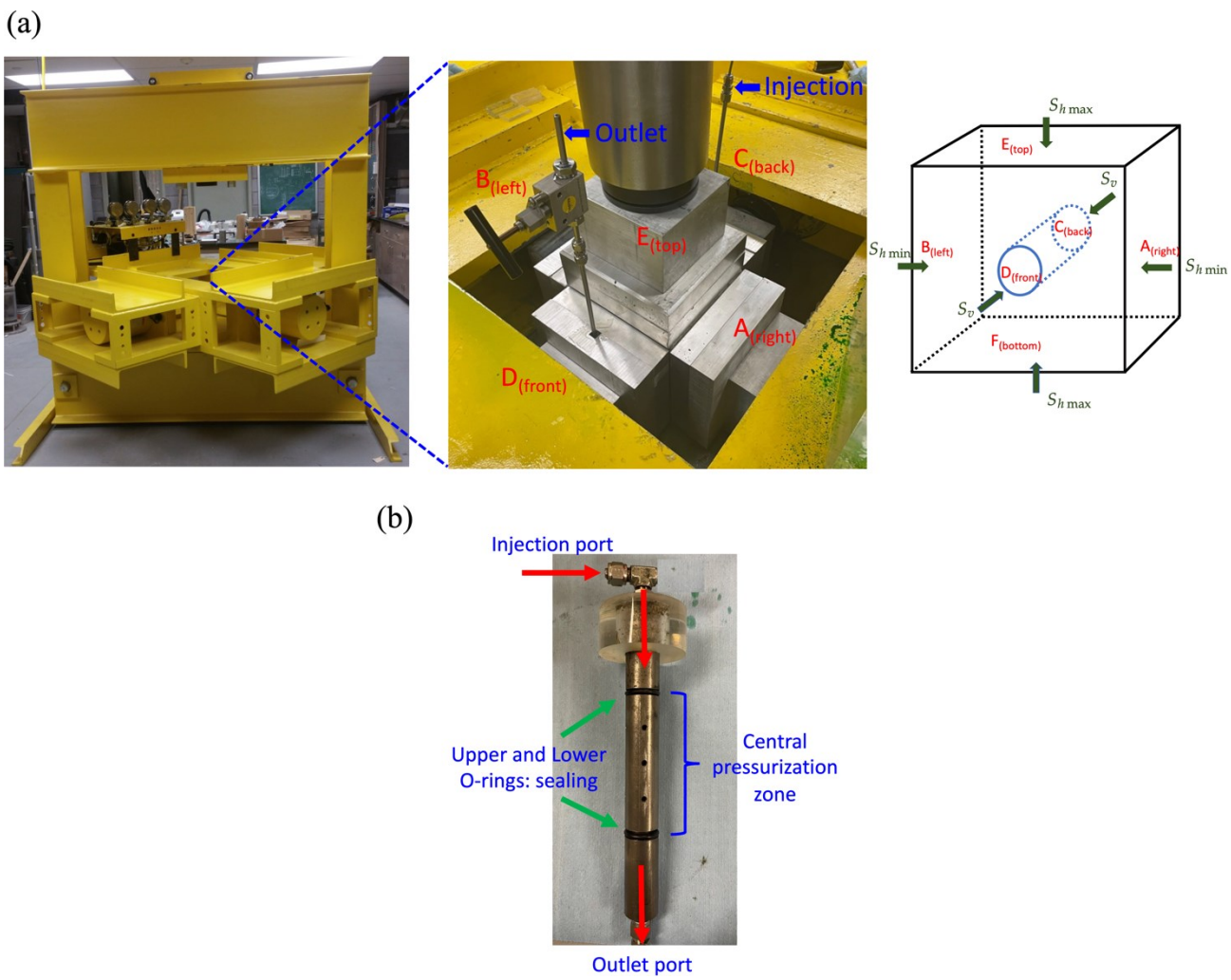

Figure 1: Experimental setup: (a) Triaxial loading frame (left) and cell (middle), and illustrations of directions of the wellbore and confining stresses (right); (b) a novel borehole injection system that utilizes two O-rings to create the seal.

The fluid injection relies on a custom-made borehole injection system as presented in Figure 1(b). Here, the system utilizes two O-rings to seal the injection area. The seal is initially undersized to the hole, but is activated by application of a small axial load to the injection tool. The load exerted on the O-rings results in lateral deformation, thereby blocking the borehole and isolating the central pressurization area. The loading platens are designed to apply this small load concurrently with application of the confining stress to the specimen. This allows for the build-up of fluid pressure in the central pressurization region as the injection proceeds. This design is favorable compared to other options for isolating a section of wellbore because it enables rapid, reliable assembly.

To begin the experiment, we first load the actuator in the wellbore direction (C-D direction) with a stress of 3.44 MPa. This step is to compress two O-rings so that the central pressurization area can be isolated, noting that only a tiny fraction of the load is transferred to the injection tool because it is accommodated in a pocket in the platen that has a soft rubber inside of it. We then close the outlet port and gradually increase the wellbore pressure to 0.68 MPa. The borehole pressure is maintained for 10 minutes to check the seal integrity. Subsequently, the stress on each direction is applied incrementally with a step of 3.44 MPa until the target value is reached. This loading scheme is employed to minimize the deviatoric stress during the loading process and thereby to minimize the potential to damage the specimen as it is being loaded. The borehole pressure is closely monitored and kept at 0.68 MPa during this loading stage. Any drops in the wellbore pressure may indicate the occurrence of damage in this loading process. After the target stress condition is satisfied, the injection fluid—a red-colored dye glycerin—is pumped at a fixed flow rate of 3 ml/min via a syringe pump. Once the peak wellbore pressure (i.e., breakdown pressure) is reached, we keep the injection for 40 seconds before entering a shut-in period. During the test, data including the flow rate and borehole pressure are continuously monitored and recorded.

To observe the near-wellbore hydraulic fractures after the test, we use an over-coring method to extract a cylinder with 3.5 inch in diameter that contains the borehole. The injection system is then reinstalled onto the cylinder and clean water is injected under a constant borehole pressure of 70 psi. The clean water penetrates preferentially through the newly created hydraulic fractures and emerges on the cylinder surface, allowing us to locate tiny hydraulic fractures that may not otherwise be visible.

2.2 Experimental Results

Figure 2 presents the evolution curves of the wellbore pressure for both Test 1 and Test 2. In both tests, the wellbore pressure first increases linearly as the injection begins and subsequently, it experiences a significant drop right after the breakdown pressure due to the initiation of hydraulic fractures. The breakdown pressure of Test 1 is approximately 28.4 MPa and that of Test 2 is approximately 19.3 MPa. After the initiation of hydraulic fractures, the wellbore pressure increases again slowly until the injection is halted. Later, the system enters a shut-in state until the confining stress is fully retracted, resulting in a decrease of the wellbore pressure to ambient.

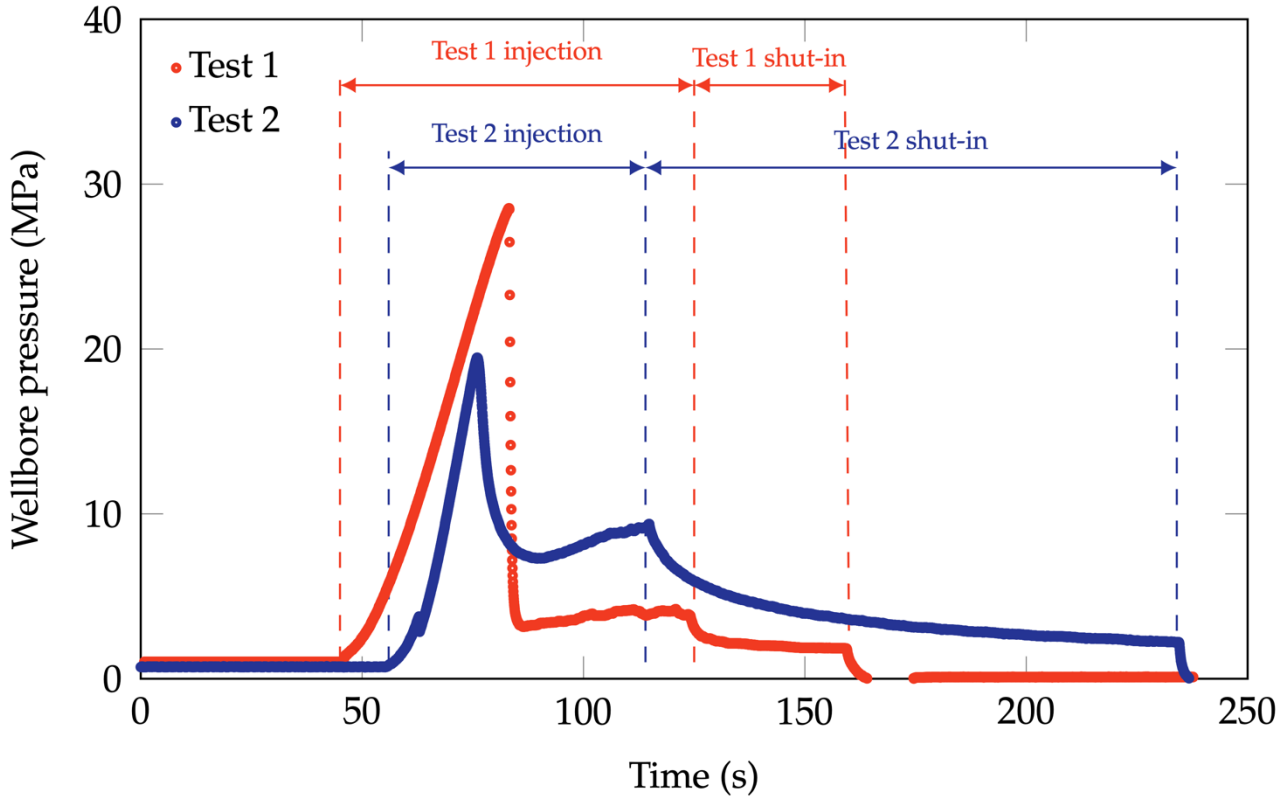

Figure 2: The wellbore pressure data for Test 1 and Test 2.

The hydraulic fractures emerged on the extracted cylinder through the water-penetration-trace method are displayed in Figure 3 and Figure 4 for Test 1 and Test 2, respectively. As illustrated in Figure 3, a total of 9 hydraulic fractures are identified in Test 1 where the borehole is drilled along the minimum wave speed direction. Six of them (Fractures 1-5 and 9) are striking the direction of the maximum horizontal stress, and hence with their opening opposed by the minimum stress (as expected from classical fracture mechanics considerations). However, most of these are inclined to the vertical direction in a manner that could indicate presence of a weaker direction promoting breakage of the rock along the transverse direction to the well. Similarly, Fractures 6 and 7 are inclined and striking at an angle of 135° from the direction of the minimum horizontal stress. Fracture 8 is in the direction of the minimum horizontal stress (i.e. nominally opposed by the maximum horizontal stress).

In contrast, Figure 4 shows simple fracture geometry with a total of 3 hydraulic fractures in a bi-wing formation resulting from Test 2 where the borehole is drilled along the maximum wave speed direction. All fractures are nearly vertical, and Fractures 1 and 2 strike at an angle of 45° from the direction of the minimum horizontal stress, while Fracture 3 strikes an angle of 225° from the direction of the minimum horizontal stress.

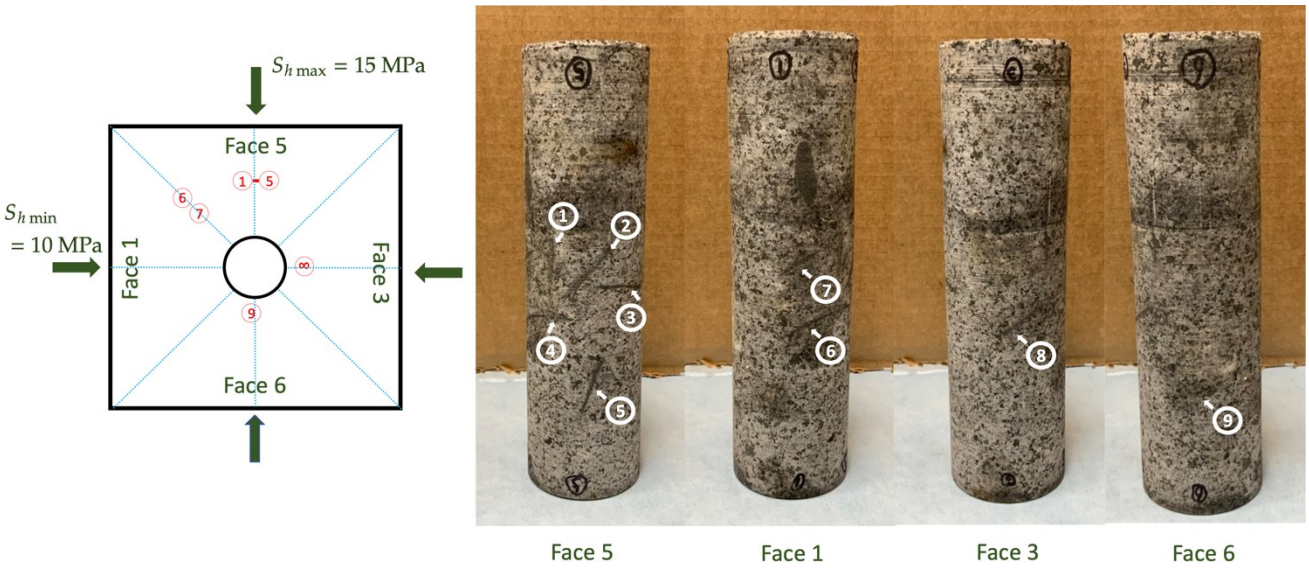

Figure 3: Observations of the hydraulic fractures through the water-penetration-trace method in Test 1.

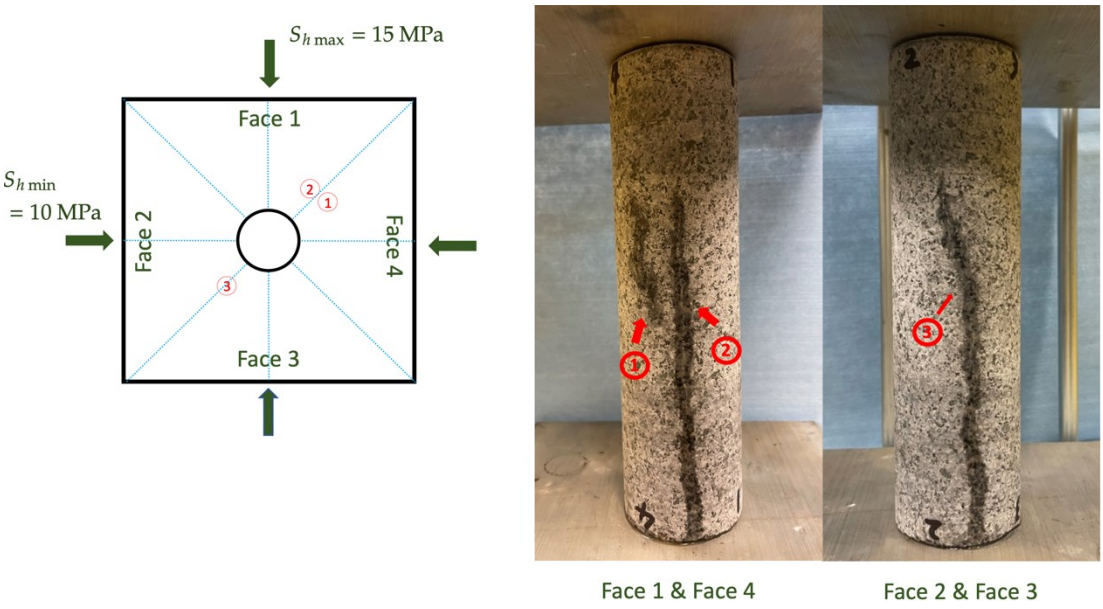

Figure 4: Observations of the hydraulic fractures through the water-penetration-trace method in Test 2.

The results indicate that hydraulic fracture initiation can be impacted by both applied stresses and the anisotropy of the granite. Most notably, the initiation generates a simpler geometry when the well is drilled along the direction of maximum wave speed, possibly indicating that the more complicated geometry obtained when drilling along the direction of minimum wave speed is related to competition between either elastic or strength related anisotropy with the tendency the fracture would otherwise have to initiate as dictated by stresses. Ongoing experiments are aimed at establishing clear tendencies of fracture initiation geometry when the wellbore is drilled in various orientations relative to both material anisotropy and principal stress axes.

3. NUMERICAL INVESTIGATION

In this section, we numerically explore the near-wellbore hydraulic fracturing process using a phase-field approach to nucleation and propagation of hydraulic fractures. We first recapitulate the ideas and features of this phase-field method, which specializes in modeling nucleation of hydraulic fractures from a smooth wellbore boundary. We then calibrate the model against experimental results of Test 1 presented in Section 2 and illustrate the ability of the phase-field model to predict the fracture nucleation behavior that is characterized by rock strengths. Then, we conduct a numerical study to investigate how the in-situ stress may affect the nucleation and propagation of hydraulic fractures.

3.1 Phase-Field Formulation and Model Calibration

In this subsection, we provide a brief description of the phase-field formulation employed in this work. In general, phase-field approximates a discrete fracture with a continuously distributed damage variable d, whose values range from 0 (intact) to 1 (fully fractured/damaged). Thus, the propagation of a phase-field fracture is naturally represented by the evolution of the damage variable according to a fracture-mechanics-based equation, which is easy to solve with a standard low-order finite element method (FEM).

To properly model hydraulic fracture nucleation and propagation from the borehole surface, we apply a new phase-field approach that was recently developed by some of the authors of this work inspired by the work of Kumar et al. (2020). This approach has incorporated stress-based ingredients into the originally purely energetic phase-field formulation for hydraulic fracturing, such that it can accurately capture fracture nucleation due to attaining the rock strength limit. In this new method, we solve the following equation that governs damage evolution,

$$-2(1-d)W^e(\varepsilon) - m'(d)bp\nabla\cdot u + m'(d)\nabla\cdot(pu) + \frac{3\mathcal{G}_c}{8L}[1 - 2L^2\nabla^2 d] + c_e = 0. \tag{1}$$

Here, $W^e(\boldsymbol{\varepsilon})$ is the strain energy of an intact material with $\boldsymbol{\varepsilon}$ denoting the strain tensor of a displacement field $\boldsymbol{u}$, $m(d)$ is a damage-dependent function, p is the fluid pressure, b is the Biot coefficient, G_c is the critical fracture energy, and L denotes the phase-field regularization length parameter. The remaining term c_e is an external driving force term that accounts for the strength of materials. Remarkably, with a specific choice for c_e and a well-designed $m(d)$ function, Equation (1) can incorporate failure (fracturing) due to a given stress-based criterion for rocks, thus allowing for an accurate prediction of the stress state near the wellbore when hydraulic fractures nucleate and propagate. In this study, we choose the expression of c_e for the Drucker–Prager criterion. More details of the model can be found in Kumar et al. (2020).

Using the above phase-field model, we perform a numerical simulation of Test 1 described in Section 2. In the simulation, we impose a prescribed pressure boundary condition $p_{\text{inj}}(t)$ on the borehole surface to model fluid injection, and the evolution of $p_{\text{inj}}(t)$ is plotted in Figure 5 according to the experimental data of Test 1. Table 1 provides the material parameters adopted in the simulation, which are calibrated to match the fracture initiation pressure obtained in Test 1. Remark that all material parameters are within realistic ranges for granite. We choose a regularization length $L = 1$ mm and an element size h that satisfies $L/h > 4$ for numerical accuracy. The initial time step size is $\Delta t = 1$ s and we further reduce it to $\Delta t = 0.02$ s once hydraulic fractures nucleate at the borehole surface.

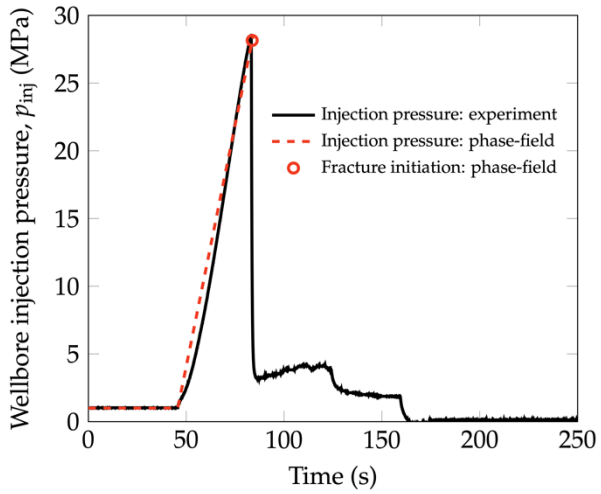

Figure 5: Injection pressure and fracture initiation pressure in model calibration.

Table 1: Material parameters used in the phase-field modeling of hydraulic fracturing in a granite sample

Parameter	Value	Unit
Bulk modulus	25.7	GPa
Shear modulus	16.4	GPa
Critical fracture energy	10.0	J/m^2
Tensile strength	13.0	MPa

Compressive strength	120.0	MPa
Biot coefficient	0.8	-
Fluid viscosity	10^{-9}	MPa·s
Fluid compressibility	0	GPa^{-1}
Initial porosity	0.05	-
Bulk permeability	10^{-9}	mm^2

As plotted in Figure 5, the phase-field method can well predict the fracture initiation pressure observed in the experiment with the calibrated parameters. Figure 6 and Figure 7 display a two-dimensional (2D) sectional view (at the plane of $z = 100$ mm) and a fully three-dimensional view, respectively, for the phase-field fracture evolution at different values of p_{inj}. Consistently with fracture mechanics theory, hydraulic fractures nucleate at the borehole surface and further propagate along the x-axis, which is the direction normal to the minimum horizontal stress $S_{h\,min}$ the injection pressure increases. These simulation results demonstrate that the phase-field model can appropriately capture the nucleation and propagation of hydraulic fractures from the borehole surface.

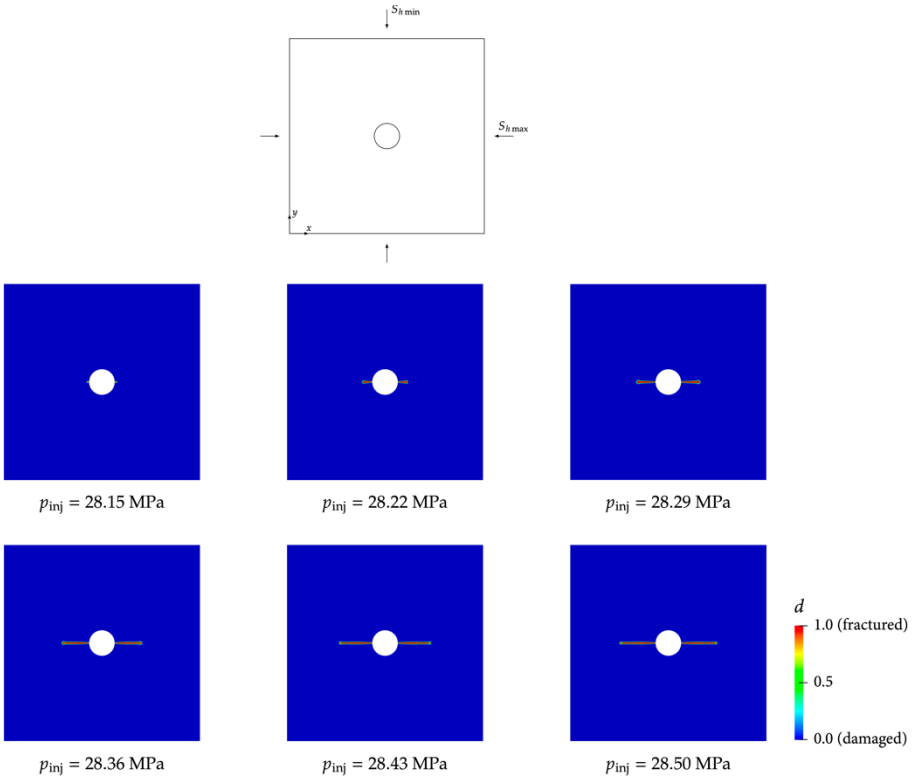

Figure 6: 2D view of the phase-field damage evolution at $z = 100$ mm obtained by model calibration

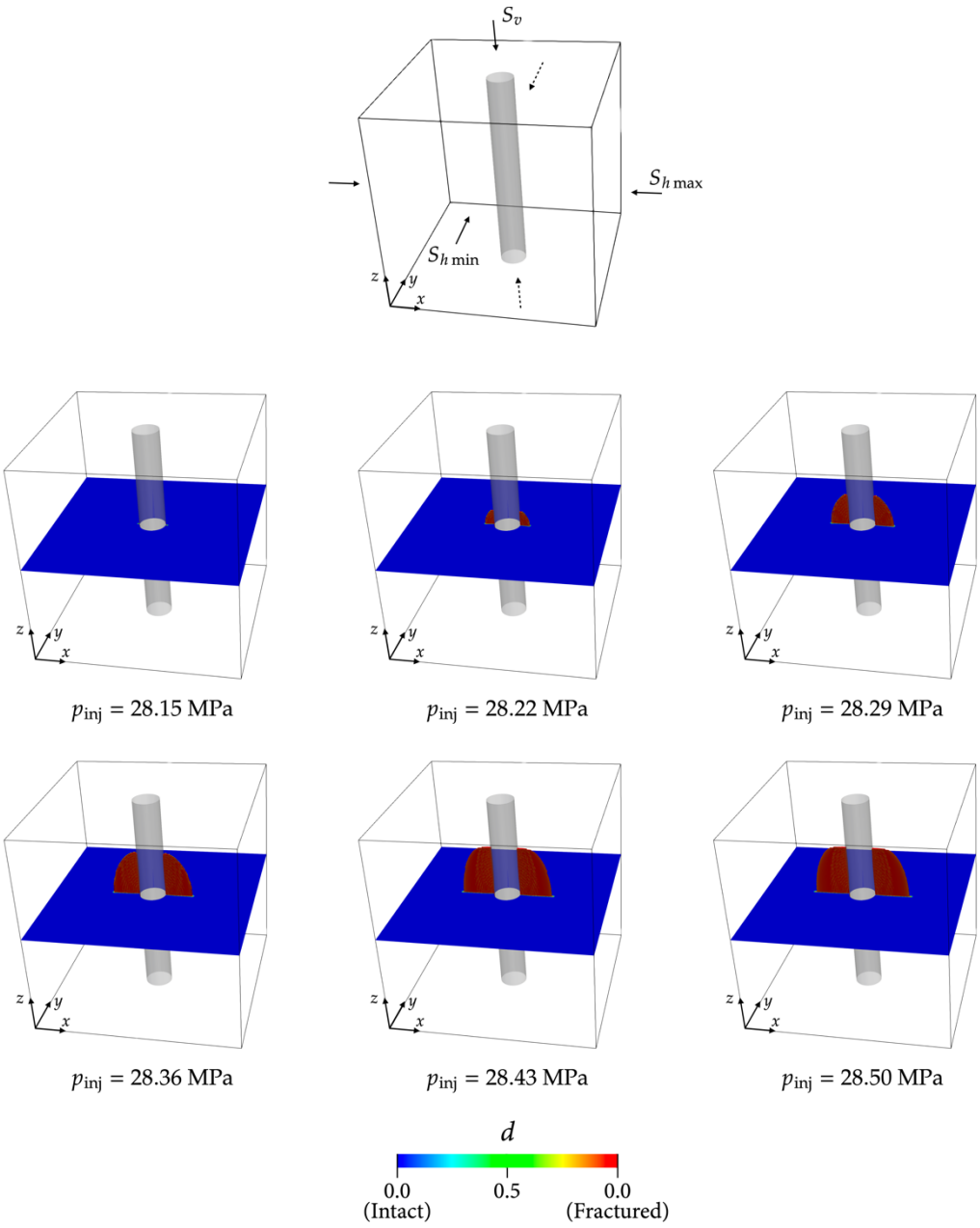

Figure 7: 3D view of the phase-field damage obtained by model calibration

3.2 Simulation with Different In-Situ Stresses

Having calibrated the phase-field model, we employ it to study the effects of in-situ stresses on the near-wellbore hydraulic fracturing pattern and the breakdown pressure. Given that the in-situ stresses used in the experiment and model calibration lie in a normal stress regime ($S_{h\,\min} < S_{h\,\max} < S_v$), we resimulate the hydraulic fracturing experiment under two other stress regimes, namely, $S_{h\,\min} = 10.0$ MPa, $S_{h\,\max} = 15.0$ MPa, and $S_v = 12.5$ MPa for a strike-slip condition, and $S_{h\,\min} = 10.0$ MPa, $S_{h\,\max} = 15.0$ MPa, and $S_v = 8.0$ MPa for a reverse condition. Remark that we only change the vertical stress while fixing two horizontal stresses.

Figure 8 presents the results of hydraulic fracture propagation for all stress regimes in both 2D view and 3D view. Remark that, as expected for a homogeneous domain, the near-wellbore hydraulic fractures always have a bi-wing planar form independently of the value of the vertical stress. This observation indicates that the in-situ stress regime has little influence on the fracture pattern for this particular setup.

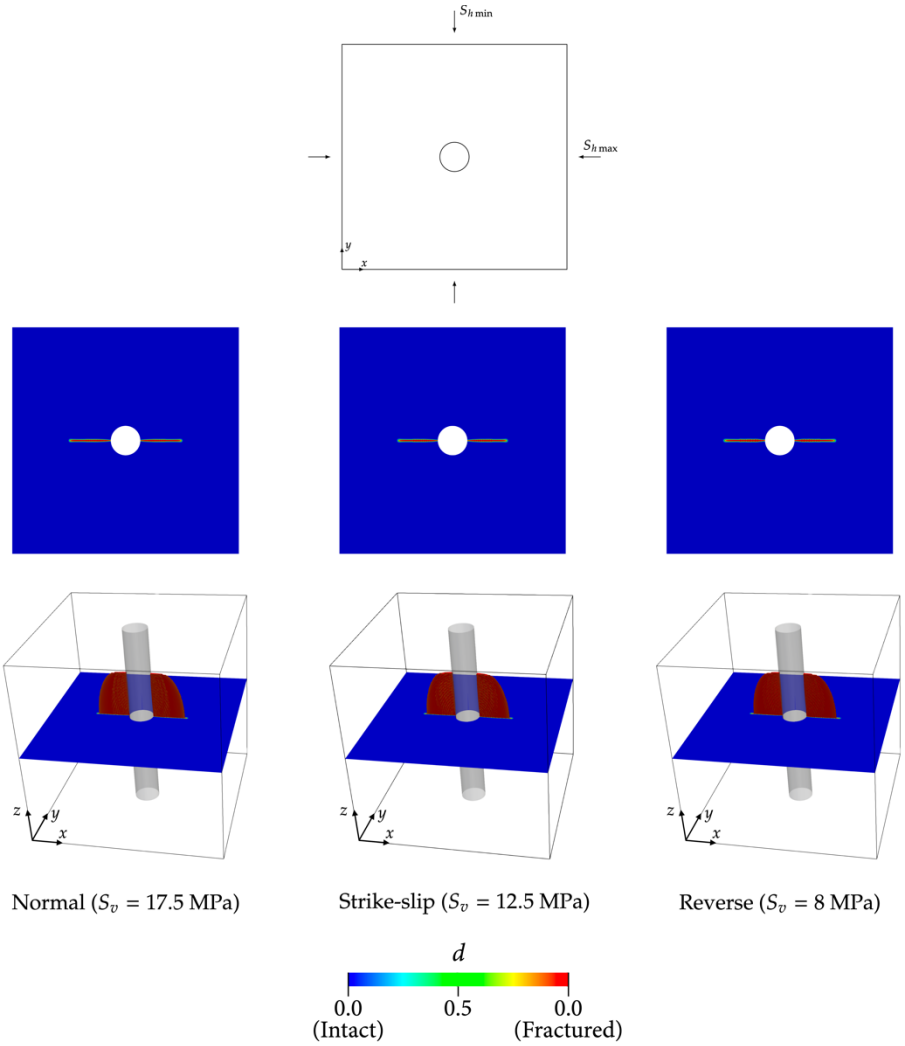

Figure 8: Phase-field results of near-wellbore hydraulic fracturing for the cases under different in-situ stress regimes.

We further compare the fracture initiation pressure for the cases with various vertical stresses S_v. Figure 9 shows a clear trend that the fracture initiation pressure increases with the vertical stress. It can be explained by the fact that a larger S_v gives a higher confining pressure, thus strengthening the granite sample according to the Drucker–Prager criterion incorporated in the formulation (1).

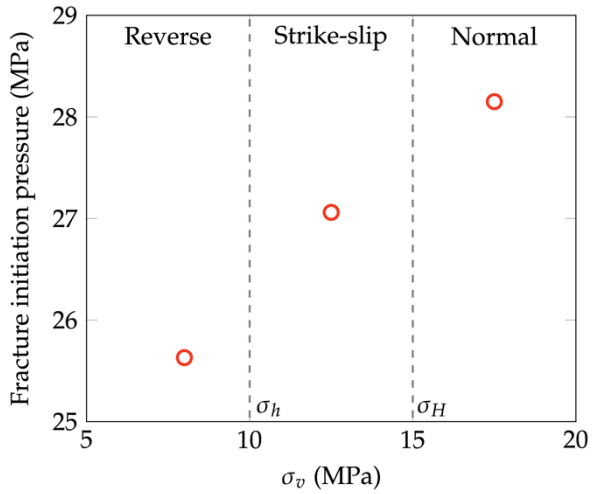

Figure 9: Phase-field results of the fracture initiation pressure for the cases under different in-situ stress regimes.

4. CONCLUSIONS

We have presented our preliminary results of a combined experimental and numerical study of the near-wellbore hydraulic fracturing process. Early laboratory experiments illustrate that we can successfully create near-wellbore hydraulic fractures in experiment by employing an advanced triaxial loading frame and a novel injection system. Different fracture patterns were observed in the samples depending on the perforation direction. This suggests the presence of stress and material properties anisotropy strongly influence the near-wellbore fracture propagation patterns. We have then used the borehole pressure data collected during the experiment to calibrate a phase-field model for hydraulic fracture nucleation and propagation. Simulation results demonstrate that this phase-field method can accurately model hydraulic fracture nucleation and propagation under varying stress conditions. We believe that this combined experimental and numerical capabilities can serve as a valuable mean to improve our understanding of the near-wellbore hydraulic fracturing process in EGS. Ongoing research activities focus on including heterogeneities in the numerical model to qualitatively reproduce the complex patterns observed in the experimental results. Future studies will include the application of this combined experimental-numerical approach to explore the influence of other factors (e.g., borehole orientation) on the near-wellbore hydraulic fracturing process.

ACKNOWLEDGEMENTS

This work relied on the GEOSX simulation framework, and the authors wish to thank the GEOSX development team for their contributions. The authors thank Utah FORGE for the financial support. This work was performed under the auspices of the U.S. Department of Energy by Lawrence Livermore National Laboratory under Contract DE-AC52-07NA27344.

REFERENCES

Borden, M. J., Verhoosel, C. V., Scott, M. A., Hughes, T. J., and Landis, C. M.: A phase-field description of dynamic brittle fracture, *Computer Methods in Applied Mechanics and Engineering, 217*, (2012), 77-95.

Chukwudozie, C., Bourdin, B., and Yoshioka, K.: A variational phase-field model for hydraulic fracturing in porous media, *Computer Methods in Applied Mechanics and Engineering, 347*, (2019), 957–982.

Cleary, M. P., Johnson, D. E., Kogsboll, H. H., Owens, K. A., Perry, K. F., De Pater, C. J., Stachel, A., Schmidt, H., and Mauro, T.: Field implementation of proppant slugs to avoid premature screen-out of hydraulic fractures with adequate proppant concentration, *Low permeability reservoirs symposium*, (1993).

Fei, F., and Choo, J.: A phase-field model of frictional shear fracture in geologic materials, *Computer Methods in Applied Mechanics and Engineering, 369*, (2020), 113265.

Fei, F., and Choo, J.: Double-phase-field formulation for mixed-mode fracture in rocks, *Computer Methods in Applied Mechanics and Engineering, 376*, (2021), 113655.

Haimson, B., and Fairhurst, C.: Initiation and extension of hydraulic fractures in rocks, *Society of Petroleum Engineers Journal, 7*(03), (1967), 310-318.

Hossain, M. M., Rahman, M. K., and Rahman, S. S.: Hydraulic fracture initiation and propagation: roles of wellbore trajectory, perforation and stress regimes, *Journal of Petroleum Science and Engineering, 27*, (2000), 129-149.

Kumar, A., Bourdin, B., Francfort, G. A., and Lopez-Pamies, O.: Revisiting nucleation in the phase-field approach to brittle fracture, *Journal of the Mechanics and Physics of Solids, 142*, (2020), 104027.

Lee, S., Wheeler, M. F., and Wick, T.: Pressure and fluid-driven fracture propagation in porous media using an adaptive finite element phase field model, *Computer Methods in Applied Mechanics and Engineering, 305*, (2016), 111-132.

Miehe, C., Welschinger, F., and Hofacker, M.: Thermodynamically consistent phase-field models of fracture: Variational principles and multi-field FE implementations, *International Journal for Numerical Methods in Engineering, 83*, (2010), 1273-1311.

Mikelic, A., Wheeler, M. F., and Wick, T.: A quasi-static phase-field approach to pressurized fractures, *Nonlinearity, 28*(5), (2015), 1371.

Santillan, D., Juanes, R., and Cueto-Felgueroso, L.: Phase field model of hydraulic fracturing in poroelastic media: Fracture propagation, arrest, and branching under fluid injection and extraction, *Journal of Geophysical Research: Solid Earth, 123*(3), (2018), 2127–2155.

Wheeler, M. F., Wick, T., and Wollner, W.: An augmented-Lagrangian method for the phase-field approach for pressurized fractures, *Computer Methods in Applied Mechanics and Engineering, 271*, (2014), 69–85.

Zhang, X., Jeffrey, R. G., Bunger, A. P., and Thiercelin, M.: Initiation and growth of a hydraulic fracture from a circular wellbore, *International Journal of Rock Mechanics and Mining Sciences, 48*, (2011), 984--995.